Final Scientific/Technical Report
Submitted to:
U.S. Department of Energy, National Energy Technology Laboratory on 6/29/2023

Tunable Rapid Uptake Amino Polymer Aerogels for Direct Air Capture of Carbon Dioxide
Award DE-FE0031951
Project Period: 2/16/2021 – 8/15/2022 (extension to 3/31/2023)

Recipient Organization:
Palo Alto Research Center
3333 Coyote Hill Rd.
Palo Alto, CA 94304
UEI Number S2VPZDS5W6M3

Principal Investigator:
Jonathan E. Bachman, Ph.D.
Research Scientist
jbachman@parc.com

Acknowledgement of Federal support:

This material is based upon work supported by the Department of Energy under Award Number DE-FE0031951.

Executive Summary:

The Palo Alto Research Center (PARC) developed a novel CO_2 adsorbent material, and in collaboration with Lawrence Livermore National Laboratory (LLNL), demonstrated its state-of-the-art performance for direct air capture. The target application for this technology is in direct air carbon capture and storage (DACCS), for which the adsorbent material provides the critical function of binding CO_2 from ambient air. At the beginning of the project, the technology concept and application were established, representing technology readiness level (TRL) 2. The hypothesis was that a microporous polymer comprising a high density of primary amines would make an exceptional adsorbent for direct air capture, and the goal of the project was to prove that hypothesis and advance the technology to TRL 3. To accomplish this, we approached the challenge from the perspective of materials synthesis optimization with the narrow focus of achieving the target material properties. This approach was successful, and we now have a synthetic procedure that results in a novel adsorbent material with the target material properties. The chemical name for the novel adsorbent material is poly(vinylamine-co-divinylbenzene) (PVAm-DVB).

The key performance metrics used to evaluate PVAm-DVB were the CO_2 adsorption capacity, CO_2 adsorption kinetics, and oxidative stability. PVAm-DVB met or exceeded all performance targets that were initially established, achieving a CO_2 adsorption capacity of 4 mmol $CO_2/g_{sorbent}$ and a CO_2 adsorption rate of 0.15 mmol $CO_2/g_{sorbent}$/min under ambient conditions (400 ppm CO_2, 75% relative humidity, 30 ˚C). The adsorption capacity and adsorption kinetics were characterized using transient breakthrough analysis. Oxidative stability was tested using an accelerated degradation experimental approach in order to simulate long-term cyclic performance of the material under real conditions. Based on these accelerated degradation studies, we project a cyclic capacity fade of < 0.01%/cycle, which is a ~6X reduction in oxidative degradation rate relative to the benchmark material.

These performance characteristics far exceed those of benchmark materials. The benchmark materials studied throughout the project were polyethyleneimine supported on silica[1] (PEI-SBA) and the commercially available, weak base anion exchange resin Lewatit VP OC 1065®[2] (Lewatit). We project that the material properties will dramatically reduce the cost of direct air capture. We estimate a capture cost of $170/net ton CO_2 removed, which is a nearly 60% reduction relative to the cost projection using the existing material's performance. We speculate that further reductions in capture cost, to the level of < $100/net ton CO_2 removed, can be achieved through additional improvements in adsorbent performance alongside cost-reductions from economies of scale.

Summary of Project Activities:

First, the key experimental evidence that validates the critical functions of PVAm-DVB are given, demonstrating TRL 3. Then, a task-by-task breakdown of project activities is given.

Experimental Validation of the Adsorbent's Critical Functions, Demonstrating TRL 3:

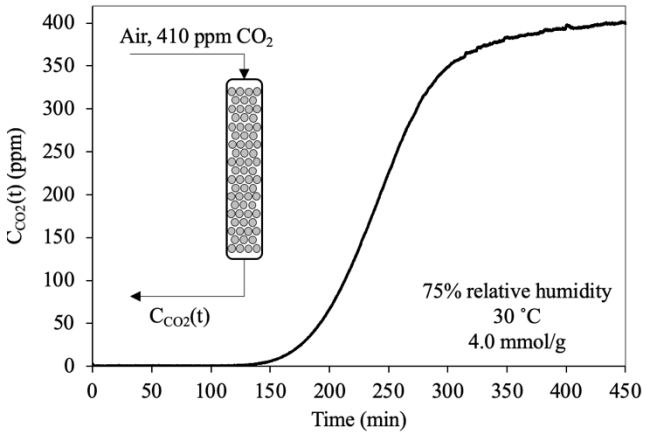

Figure 1: Transient breakthrough analysis demonstrating an equilibrium **adsorption capacity of 4.0 mmol $CO_2/g_{sorbent}$**. The experiment was conducted under 75% relative humidity and 30 ˚C, flowing 410 ppm CO_2 in N_2.

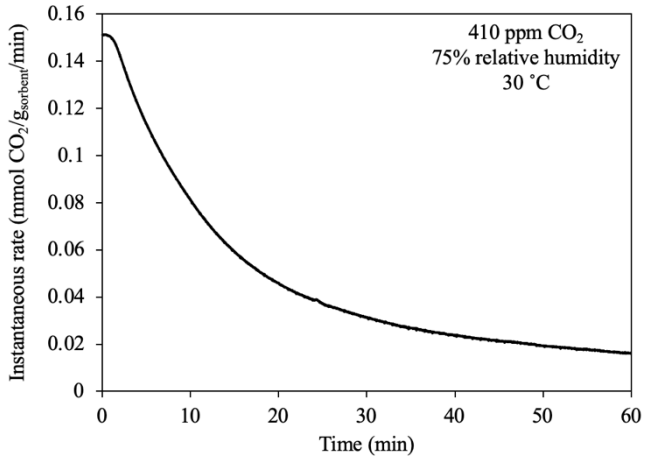

Figure 2: Transient breakthrough analysis demonstrating an **adsorption rate of 0.15 mmol $CO_2/g_{sorbent}$/min**. The experiment was conducted under 75% relative humidity and 30 ˚C, flowing 410 ppm CO_2 in N_2.

Table 1: Results from an accelerated aging study, comparing PVAm-DVB with Lewatit, after exposure to O_2 at 100 ˚C for 8 h, demonstrating a predicted **capacity fade of 0.01%/cycle** for PVAm-DVB.

		O_2 concentration	
Parameter	Material	21%	14%
Degradation rate (%/min)	PVAm-DVB	0.0062%	0.0007%
	Lewatit	0.0112%	0.0041%
Capacity fade (%/cycle)	PVAm-DVB	0.09%	**0.01%**
	Lewatit	0.17%	0.06%

Summary of Tasks and Milestones:

The project occurred in one budget period and was divided into 6 tasks: Project management and planning (Task 1), Develop aerogel formulations (Task 2), Lab-scale aerogel characterization to support materials development (Task 3), Aerogel scale-up and physical characterization (Task 4), Fixed-bed sorbent testing (Task 5), and Conceptual DAC process design and evaluation (Task 6). A summary of the milestones, including their corresponding subtask, description, and actual completion date are shown in Table 2.

Table 2: Milestone table.

Subtask	Milestone Description	Completion Date
2.1	Produce a porous aerogel with baseline amine content	11/30/2021
2.2	Produce a porous aerogel with target amine content	5/31/2022
3.2	Sub-gram characterization of Initial aerogel showing that it is feasible to achieve Initial State Point oxidative stability, equilibrium loading and kinetics.	4/14/2022
3.2	Sub-gram characterization of Target aerogel showing that it is feasible to achieve Target State Point oxidative stability, equilibrium loading and kinetics.	10/30/2022
4.1	Produce aerogel at fixed bed testing, capable of achieving Initial State Point equilibrium loading, kinetics, and oxidative stability	2/28/2022
4.2	Measure all *sorbent* properties in the State Point Table for the Target aerogel formulation, except Capacity retention, 10 cycles.	12/31/2022
5.1	Measure and compare properties of candidate materials received Q1-Q4	5/31/2022
5.1	Demonstrate that final aerogel formulation achieves Target State Point Table metrics for equilibrium loadings, kinetics, and report capacity retention over repeated cycling.	3/20/2023
5.2	Propose process parameters (regeneration method, regeneration temperature, cycle time) for the most promising sorbent	11/30/2022
6.1	Create top-level Process Flow Diagram (PFD)	1/27/2022
6.2	Identify material and process parameters that most drive overall system cost	5/31/2022
6.2	Update cost assessment based on process parameters determined in M5.2	12/20/2022

Task 2: Develop Aerogel Formulations

The goal of Task 2 was to develop and optimize the synthesis of the amino-polymer. This task was divided into the demonstration of an amino-polymer with a 'baseline' amine content of greater than 45 wt.% of amine-containing monomer and then the demonstration of an amino-polymer with a 'target' amine content of greater than 75 wt.% of amine-containing monomer.

Table 3: Task 2 milestone descriptions.

Subtask	Milestone Description	Completion Date
2.1	Produce a porous aerogel with baseline amine content	11/30/2021
2.2	Produce a porous aerogel with target amine content	5/31/2022

While achieving the baseline and target formulations were objectives of Task 2, the overarching goal was to optimize the formulation to maximize CO_2 adsorption capacity. At the outset of the project, the optimal amine-loading was unknown, so the baseline and target formulations of 45 and 75% were arbitrary, and served more as demonstrations that the amine loading could be controlled. During the early work on Task 2, the general synthesis route was identified. The synthesis involves the polymerization of vinylformamide with divinylbenzene to produce poly(vinylformamide-co-divinylbenzene), followed by an acid deprotection and base neutralization to form poly(vinylamine-co-divinylbenzene) (PVAm-DVB). The conceptual and actual synthesis schemes for amino-polymer synthesis is shown in Figure 3.

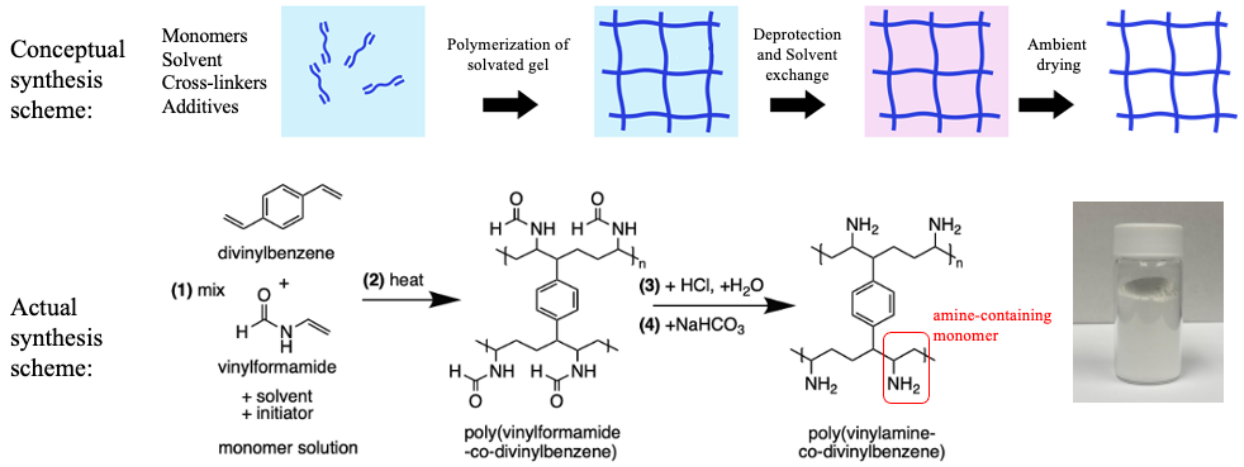

Figure 3: Conceptual (top) and actual (bottom) synthesis schemes for producing PVAm-DVB. The synthesis involves (1) mixing the monomers, solvent, and initiator to create the monomer precursor solution, (2) polymerizing the mixture, (3) acid deprotection of formamide to ammonium moieties, and (4) base neutralization of the ammonium moieties to amines. The synthesis is followed by drying to form the PVAm-DVB powder.

The formulation was optimized across several parameters, including the polymerization time, polymerization temperature, monomer ratio, initiator type and concentration, solvent concentration, deprotection reagent type and concentration, deprotection time, neutralization agent, and drying conditions. Each of these parameters were systematically studied to understand their effect on the resulting material's structure, composition, and performance. Different reaction conditions yielded materials with various compositions (i.e., mass fractions of amine-containing monomer), structure (i.e., surface area, pore volume, and pore size distribution), and performance (i.e., CO_2 adsorption capacity).

The range of compositions attained and the methods for measuring polymer composition are discussed here. The amine loading in the polymer was determined based on CHNO elemental analysis, performed by Midwest Microlabs, Inc. The raw elemental analysis data comprises wt.% C, wt.% H, wt.% N, and wt.% O. The wt.% amine-containing segment was then determined based on the element molar ratio determined from elemental analysis and the monomer's elemental composition. The amine-containing segment in the polymer has the repeat unit $–CH_2CHNH_2–$ corresponding to a vinylamine unit with a molecular weight of 43.06 g/mol, 1 N and 2 C. The cross-linking segment in the polymer has the repeat unit $-CH_2CHC_6H_6CHCH_2–$, corresponding to

a divinylbenzene unit with a molecular weight of 130.19 g/mol, 0 N and 10 C. Therefore, the observed C:N ratio yields a wt.% of amine containing monomer. Throughout the course of the formulation optimization, > 100 samples were characterized via elemental analysis. A summary of the elemental analysis results is shown in Figure 4.

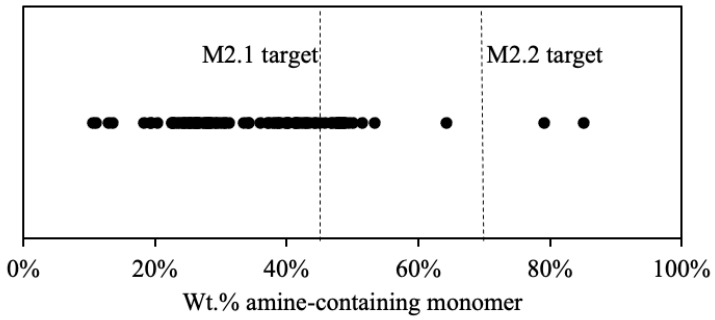

Figure 4: Summary of elemental analysis results collected over the course of the project. The raw element wt.% were converted to wt.% amine-containing monomer using the C:N ratio and the monomer formulas. The M2.1 target of 45 wt.% and M2.2 target of 75 wt.% are shown on the dashed lines, and correspond to the "baseline" and "target" aerogel formulations, respectively.

Table 4: Elemental analysis data for two samples that meet the "baseline" and "target" formulation requirements as set out in the milestones.

	wt.% C	wt.% N	C:N	VAm:DVB	wt.% amine segment
"Baseline" formulation	65.12%	14.11%	5.38	2.96	49.4%
"Target" formulation	55.39%	22.45%	2.87	11.43	79.1%

It was found that the polymer composition can vary significantly, with amine content ranging from 10.6 wt.% to 85.1%. While the amine content can be precisely controlled, the amine's accessibility also has to be maintained in order to utilize the amine functionality for CO_2 adsorption. We found that, at very high amine loading (> 60 wt.%), the PVAm-DVB no longer had microporosity and did not adsorb CO_2.

As mentioned above, the absolute amine loading in the polymer is less important than the adsorbent's performance. In other words, the relationship between the amine loading and the CO_2 adsorption is critical. Thus, we sought to elucidate how the polymer's composition (i.e., its mmol $N/g_{sorbent}$ or wt.% amine-containing monomer) affected its performance (i.e., equilibrium CO_2 adsorption capacity). In addition to elemental composition, each sample's CO_2 adsorption capacity was also characterized. CO_2 adsorption was measured by thermogravimetric analysis (TGA). In a typical TGA experiment, 5-15 mg of sample will first be activated at 100 ˚C for 3 hours under 100% N_2. Then, the sample is cooled to 25 ˚C under 100% N_2. Finally, the adsorption measurement begins by changing the gas composition to 400 ppm CO_2, balance N_2. The mass change measured by the TGA corresponds to CO_2 adsorption. The structure-property relationships, showing the CO_2 adsorption and amine efficiency functions of the amine content are shown in Figure 5.

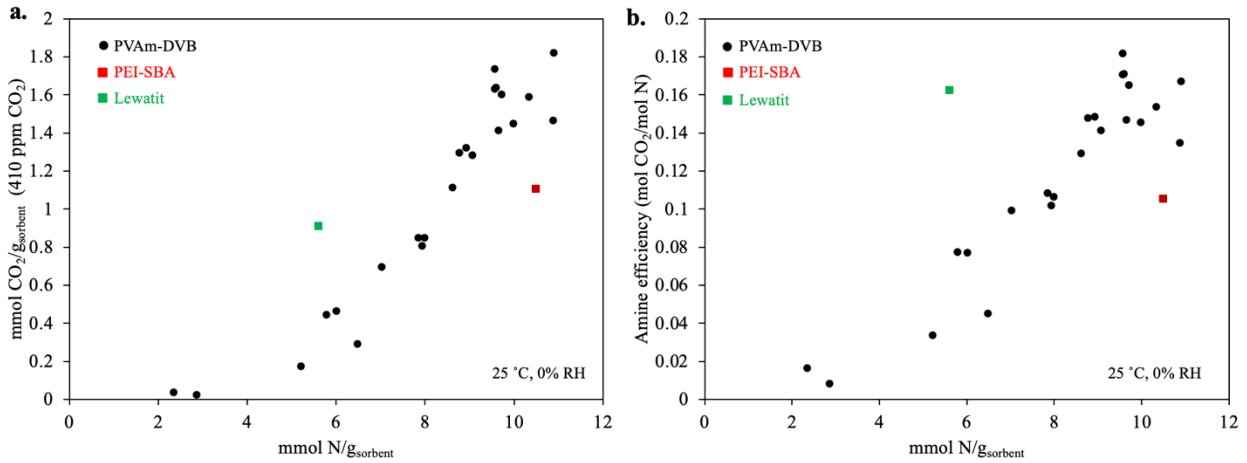

Figure 5: Structure-property relationships for CO_2 capture in PVAm-DVB (black circles), compared with the benchmark materials PEI-SBA (red squares) and Lewatit (green squares). **(a)** equilibrium adsorption (mmol $CO_2/g_{sorbent}$) vs. N loading (mmol $N/g_{sorbent}$), with adsorption measured by TGA under 0% relative humidity and 25 ˚C. **(b)** amine efficiency (mol CO_2 adsorbed/mol N) vs. amine loading (mmol $N/g_{sorbent}$).

To the best of our knowledge, this is the first such structure-property relationship that has been developed and was made possible by the extensive synthesis effort. This type of structure-property relationship can only be produced in a system where the amine loading can very continuously, i.e., in a co-polymer in which one of the monomers is amine-containing and the monomer ratio can be varied from 0% to 100%. We found a positive correlation between N loading and CO_2 adsorption, which was expected based on the adsorption mechanism – if there are more adsorption sites present in the material, more adsorption is expected to occur. More surprising was the effect of amine loading on amine efficiency. Amine efficiency is the fraction of amines that have adsorbed CO_2. For illustration, if the material comprises 10 mmol $N/g_{sorbent}$ and adsorbs 1.8 mmol $CO_2/g_{sorbent}$, then its amine efficiency is 0.18 mol CO_2/mol N. A positive correlation between amine loading and amine efficiency was found. This relationship is consistent with a > 1:1 amine:CO_2 adsorption mechanism, such that multiple amines need to be adjacent in order to bind CO_2. In that scenario, as amine loading is increased, there are more neighboring amines that can participate in CO_2 adsorption. We speculate that the influence of amine loading on amine efficiency is reduced at elevated relative humidity. Under high relative humidity, a 1:1 amine:CO_2 adsorption mechanism may become favorable.

Task 3: Develop Lab-Scale Aerogel Formulations

Table 5: Task 3 milestone descriptions.

Subtask	Milestone Description	Completion Date
3.2	Sub-gram characterization of Initial aerogel showing that it is feasible to achieve Initial State Point oxidative stability, equilibrium loading and kinetics.	4/14/2022
3.2	Sub-gram characterization of Target aerogel showing that it is feasible to achieve Target State Point oxidative stability, equilibrium loading and kinetics.	10/30/2022

The goals of Task 3 were to demonstrate the performance of the novel amino-polymer in terms of its oxidative stability, equilibrium loading, and kinetics. Initial and final performance targets were set, as shown in Table 6.

Table 6: Initial and final performance targets for Subtask 3.2.

Parameter	Units	Initial performance	Target performance
Oxidative stability*	% retention	70%	90%
Equilibrium loading	mmol $CO_2/g_{sorbent}$	1	4
CO_2 adsorption kinetics	mmol/g/min	0.10	0.15
CO_2 desorption kinetics	mmol/g/min	0.2	0.3

*defined as CO_2 capacity retention after exposure to 21% O_2 at 100 ˚C for 20 h.

The experimental evidence demonstrating the target oxidative stability, equilibrium loading, and adsorption kinetics are given in Table 1, Figure 1, and Figure 2, respectively. For the oxidative stability, the measured degradation rate under 21% O_2 and 100 ˚C was 0.0062%/min. Translating that to the defined performance units (% retention after 20 h) yields a retention of 92.56%, meeting the target performance. For the equilibrium loading, breakthrough analysis was used to demonstrate 4 mmol $CO_2/g_{sorbent}$ under 400 ppm CO_2, 30 ˚C, and 75% relative humidity. For CO_2 adsorption kinetics, breakthrough analysis was used to demonstrate a 0.15 mmol/g/min adsorption rate. For CO_2 desorption kinetics, thermogravimetric analysis was used. CO_2 desorption rate was determined by the mass loss during heating and N_2 purge. Under these conditions, an instantaneous desorption rate as high as 0.45 mmol/g/min was recorded.

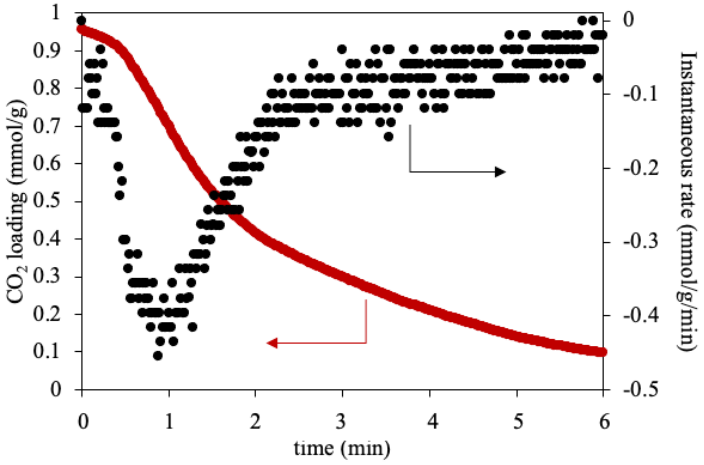

Figure 6: Thermogravimetric analysis (TGA) results for CO_2 desorption including the instantaneous CO_2 loading (mmol/g, left axis) and instantaneous CO_2 desorption rate (mmol/g/min, right axis). Desorption occurred during temperature ramp to 100 ˚C, under flowing N_2.

While the adsorption rate is limited by the CO_2 feed rate in the gas phase (i.e., the faster air is flowed, the faster CO_2 is adsorbed), the desorption rate is instead limited by heat transfer to the adsorbent (e.g., the higher the heat flux, the faster CO_2 is desorbed). Therefore, in both cases, we are observing 'extrinsic' kinetics, which are determined not by the adsorbent's properties but rather by the physical setup of the system. This is beneficial, as it indicates that the adsorbent's 'intrinsic'

kinetics (i.e., solution-diffusion limited CO_2 transport) are much higher than the target values. Thus, if the engineering design of the DAC contactor and system are optimized, very high adsorption and desorption rates are achievable.

Task 4: Aerogel Scale-up and Physical Characterization

Table 7: Milestone table for Task 4.

Subtask	Milestone Description	Completion Date
4.1	Produce aerogel at fixed bed testing, capable of achieving Initial State Point equilibrium loading, kinetics, and oxidative stability	2/28/2022
4.2	Measure all *sorbent* properties in the State Point Table for the Target aerogel formulation, except Capacity retention, 10 cycles.	12/31/2022

Since the final state point equilibrium loading, kinetics, and oxidative stability have been demonstrated earlier in this report, the focus of this section is on the measurement of sorbent properties in the state point table. Previously, PVAm-DVB was synthesized in a powder form. This was a challenge for attaining certain state point table properties including bulk density and average particle diameter (which was targeted as 'controllable'). To deal with this, a structured adsorbent approach was developed. Existing structured adsorbent platforms include monolithic, laminate, and foam structures.[3] However, the structured adsorbent approach developed here is separate and novel compared to those previous approaches, as shown in Figure 7. The new approach utilizes a non-woven mesh reinforcement. Instead of conducting a bulk polymerization within a vial or jar, the monomer solution is soaked into a non-woven polypropylene mesh. The monomer-soaked mesh is sandwiched between two plates to prevent solvent evaporation, heated to induce polymerization, and then subjected to the work-up conditions that yields the adsorbent functionality. The result is polypropylene-reinforced PVAm-DVB. This structuring approach is enabled by the radical polymerization platform, meaning that other synthetic approaches to adsorbent production (e.g., metal–organic framework crystallization) would not be compatible.

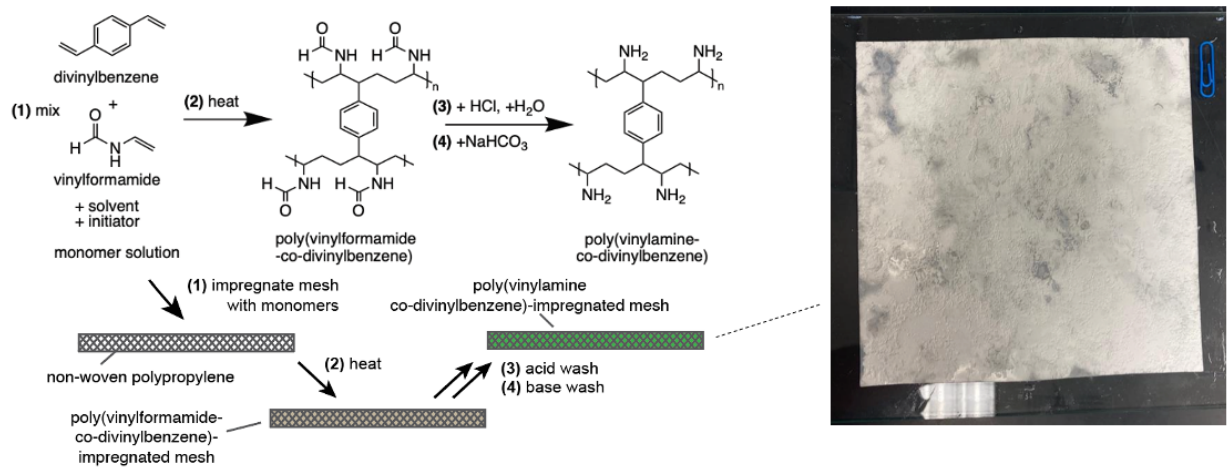

Figure 7: Structured adsorbent platform to produce polypropylene-reinforced PVAm-DVB. The chemical synthesis steps (top left) map onto the illustrative fabrication steps (bottom left). The resulting structured adsorbent is a flat sheet comprising polypropylene-reinforced PVAm-DVB (right).

Table 8: Characteristics of the structured adsorbent.

Thickness (um)	Areal density (g/m2)	Bulk density (kg/m3)	Active material loading
357.8 ± 7.0	161.1 ± 2.7	450.3 ± 7.5	81.5% ± 0.4%

The physical characteristics of an individual structured adsorbent sample are given in Table 8. Notably, the structured adsorbent had a bulk density that was ~3X higher than the adsorbent powder and had an active material (adsorbent) loading of > 80 wt.%. These are notable achievements because improving bulk density and active material loading increase the volumetric capacity, which is a key metric of an air contactor's performance.

Task 5: Fixed-bed Sorbent Testing

Table 9: Milestone table for Task 5.

Subtask	Milestone Description	Completion Date
5.1	Measure and compare properties of candidate materials received Q1-Q4	5/31/2022
5.1	Demonstrate that final aerogel formulation achieves Target State Point Table metrics for equilibrium loadings, kinetics, and report capacity retention over repeated cycling.	3/20/2023
5.2	Propose process parameters (regeneration method, regeneration temperature, cycle time) for the most promising sorbent	11/30/2022

Over the course of the project, PARC shipped samples to LLNL for fixed-bed adsorbent testing (a.k.a. breakthrough analysis), in accordance with Subtask 5.1. Generally, PARC would first screen samples using TGA, and then send samples with the highest CO_2 adsorption capacity. The breakthrough characterization by LLNL was needed to measure adsorption under humid conditions. We found that CO_2 adsorption dramatically increases under elevated relative humidity. In order to measure under a controlled relative humidity, the breakthrough system is housed in a temperature-controlled environmental chamber at elevated temperature. A temperature-controlled bubbler is used to humidify the inlet air. The CO_2 concentration at the outlet of the bed was monitored using an infrared (IR) gas analyzer.

Demonstration that the final aerogel formulation achieves Target State Point Table metrics for equilibrium loadings and kinetics was completed as discussed earlier. In order to complete Subtask 5.1 (report capacity retention over repeated cycling), the final champion material (which met the target 4 mmol/g capacity) was then characterized by fixed-bed testing over 10 cycles, as shown in Figure 8. This type of cycling experiment represents reproducibility of the breakthrough analysis procedure more than the adsorbent's intrinsic stability. The accelerated oxidation studies, as discussed previously, led to more relevant measurements of the degradation rate and cyclic capacity fade.

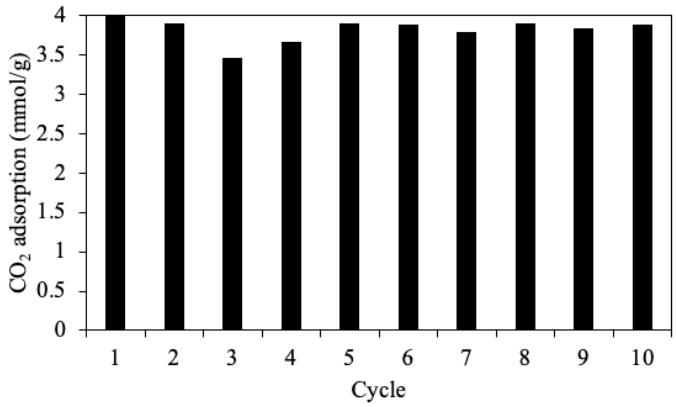

Figure 8: Transient breakthrough over repeated cycling on PARC adsorbent material. The experiment was conducted at 30 ˚C and 75% relative humidity. The material was first regenerated at 100 ˚C under flowing N_2 with 3.7 kPa of H_2O (the equivalent of 75% RH at 30 ˚C) overnight. Then, a gas mixture comprising 410 ppm CO_2, 3.7 kPa H_20, balance N_2, was flowed through the column, and the outlet CO_2 concentration was measured over time.

There were two outlier runs with earlier breakthrough times than others in the sequence that resulted from a decrease in temperature within the heated enclosure to < 30 ˚C. The decreased temperature resulted in a lower relative humidity and thus lower CO_2 adsorption for those runs. For the remainder of the runs, the transient breakthrough experiment was highly reproducible. With the capacity retention over repeated cycling now measured, the final State Point Table with measured values was completed.

For Subtask 5.1, we sought to propose operating conditions that will be energy efficient and maximize the adsorbent's lifetime. For the regeneration method, we have considered temperature-swing adsorption (TSA) system with indirect heating (e.g., using a heating element or a heating fluid), and a steam-temperature vacuum swing desorption (S-TVSD) system that uses steam condensation to provide the required heat for desorption. To assess the regeneration temperature, we considered what temperature would lead to the lowest regeneration energy. For the cycle time, we used experimental adsorption rate data collected on the sorbent. We have proposed to use a steam-temperature vacuum swing desorption (S-TVSD) system, that uses low-temperature steam for the regeneration method. The S-TVSD method enables rapid desorption via fast heating during steam condensation. The S-TVSD system does not require significant thermal conduction to occur, like in systems that use indirect heating for desorption. Additionally, we have proposed to use a desorption temperature in the range of 80-90 ˚C. This desorption temperature is consistent with the S-TVSD system, in that it utilizes sub-ambient pressure steam's saturation temperature. Finally, we propose to use a 15 minute cycle time, that is supported by adsorption rate measurements, as shown in Figure 9.

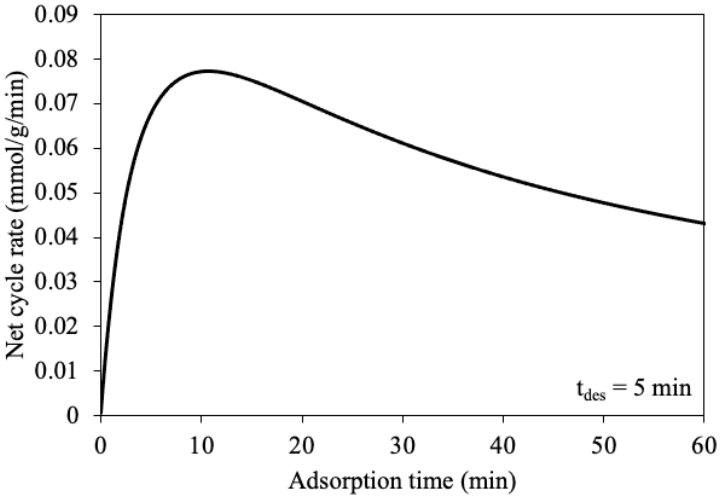

Figure 9: Net cycle rate vs. adsorption time, corresponding to the adsorption rate data shown in Figure 2 and for a fixed desorption time (t_{des}) of 5 minutes. The peak in the net cycle rate corresponds to an optimal adsorption time of 10 minutes, so that the optimal total cycle time is 15 minutes.

Other key adsorbent characteristics include the particle void fraction and packing density, which can be determined using measured porosimetry values. The cumulative pore volume was used to determine the particle void fraction, and the cumulative surface area was used to determine the packing density. These values were measured using mercury intrusion porosimetry, which enables characterization of pore sizes ranging from 2 nm to 200 um. The mercury intrusion porosimetry was conducted on the adsorbent powder, not the structured adsorbent, resulting in significant pore volume coming from pores with > 1 um pore diameter. The cumulative pore volume and cumulative surface area, as a function of pore diameter, are shown in Figure 10.

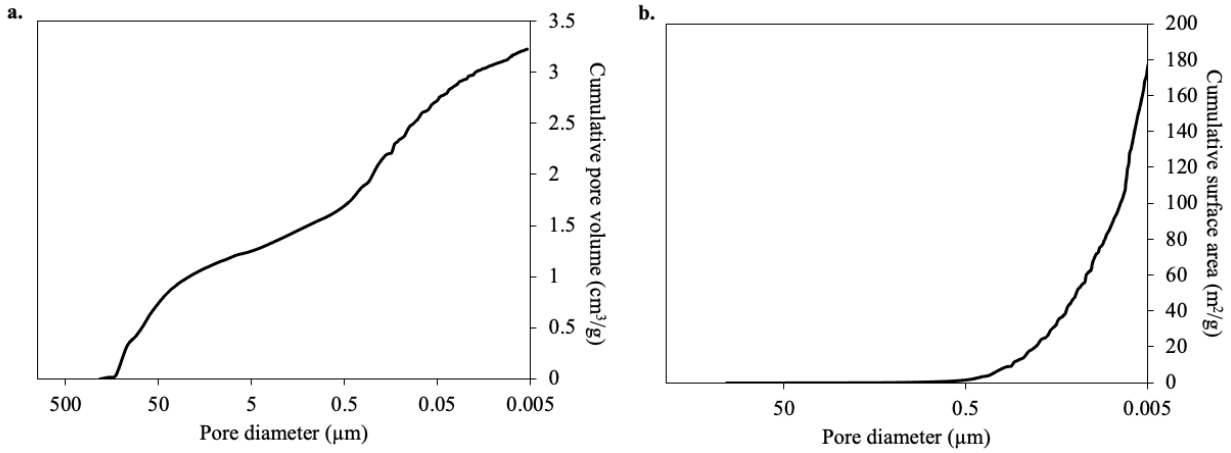

Figure 10: Cumulative pore volume **(a)** and cumulative surface area **(b)** as a function of pore diameter of PVAm-DVB powder, as measured using mercury intrusion porosimetry.

Table 10: Final State Point Table with target and measured values.

	Units	Target Value	Measured Value
Adsorbent			
True Density @ STP	kg/m^3	1000	970
Bulk Density	kg/m^3	450	450
Average Particle Diameter	mm	Controllable 0.01-30	0.36
Particle Void Fraction	m^3/m^3	0.3	0.76
Packing Density	m^2/m^3	$0.24 \cdot 10^9$	$0.04 \cdot 10^9$
Solid Heat Capacity @ STP	kJ/kg•K	1.2	1.23
Capacity Retention, 10 cycles	%	Report	97%
Oxidative Stability	% / cycle	90.00%	92.56
Adsorption			
Pressure	bar CO_2	0.0004	0.0004
Temperature	˚C	25	25
Equilibrium Loading	gmol CO_2/kg	4	4
Heat of Adsorption	kJ/gmol CO_2	45	41
CO_2 Adsorption Kinetics	mmol CO_2/g/min	0.15	0.15
Desorption			
Pressure	bar	0.5	0.5
Temperature	˚C	110	80
Equilibrium Loading	gmol CO_2/kg	0.4	0
Heat of Desorption	kJ/gmol CO_2	45	41
CO_2 Desorption Kinetics	mmol CO_2/g/min	0.3	0.4

Task 6: Conceptual DAC Process Design and Evaluation

Table 11: Milestone table for Task 6.

Subtask	Milestone Description	Completion Date
6.1	Create top-level Process Flow Diagram (PFD)	1/27/2022
6.2	Identify material and process parameters that most drive overall system cost	5/31/2022
6.2	Update cost assessment based on process parameters determined in M5.2	12/20/2022

A comprehensive technoeconomic analysis (TEA) for a DAC facility using an adsorbent was developed. The CO_2 production capacity of the modeled DAC facility was 100,000 tons/year. The objective was to develop a technoeconomic model that considered the process and adsorbent parameters learned throughout the project, and project a CO_2 capture cost for a 100,000 ton/year DAC facility. Then, we aimed to compare the projected CO_2 capture cost for a DAC facility using PARC's sorbent, to one using the same process design but instead using baseline adsorbent properties.

The envisioned DAC facility utilized a steam-temperature vacuum swing desorption (S-TVSD) process, wherein steam condensation is used to provide the latent heat needed for desorption. The S-TVSD process operates at sub-ambient pressure (0.5 bar), where the saturation temperature of steam is 83 ˚C. Steam condensation under sub-ambient pressure provides rapid heat transfer. The combination of rapid heat transfer, reduced pressure, and added sweep gas (steam) provides a large driving force for CO_2 desorption, minimizing the time required for regeneration. In addition to steam condensation, a hybrid system using hot oil was also implemented. The hot oil system is used to provide the sensible heat to the adsorbent as well as the housing and other components in the contactor, to minimize water usage in the system.

The DAC facility included 12 contactors per bank, with the number of banks being calculated based on the amount of adsorbent mass needed to achieve 100,000 ton/year capture rate. Each contactor contained 633 kg of adsorbent and had a volume of 2.8 m^3. Each contactor was equipped with an individual fan. A single steam generation unit was used to supply steam to the contactor banks. A hot oil system was envisioned to provide the sensible heat that brings the system to the desorption temperature. This is helpful to minimize water usage in the system, and supplies the heat needed to bring the non-sorbent contactor mass to the desorption temperature. Following desorption, the steam and desorbed CO_2 are flowed through a condenser and knockout drum which separates the water from the gaseous CO_2. Finally, the CO_2 is flowed through the vacuum pump which exhausts the CO_2 at ambient pressure. The process flow diagram for the DAC facility is shown in Figure 10.

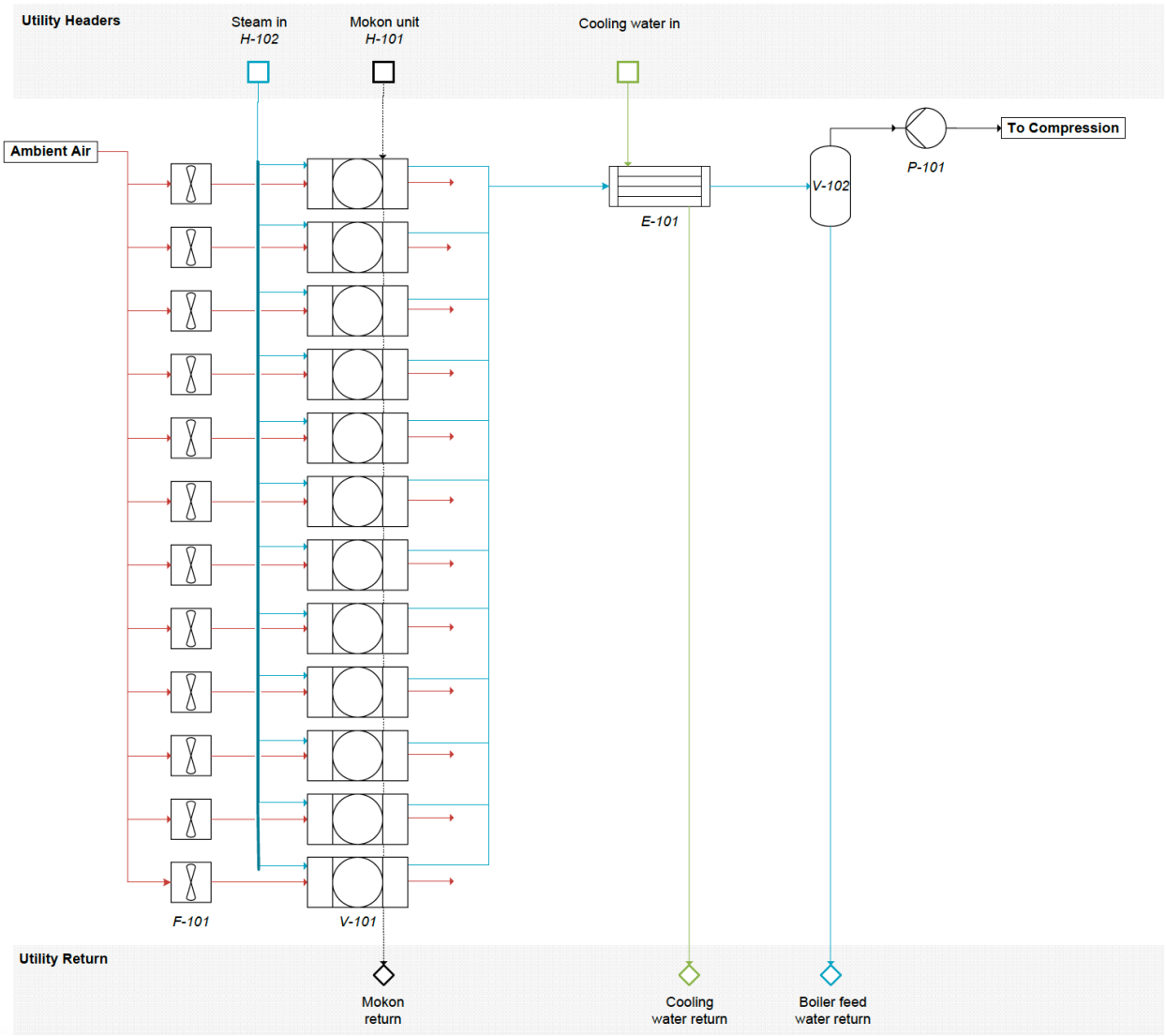

Figure 10: Process flow diagram for a 'contactor bank' using the process type detailed in milestone 5.2. Streams for adsorption are depicted in red, and streams for desorption are depicted in blue. On the adsorption side, ambient air is brought in using fans and flowed through the contactors (V-101). The pressure drop for the contactors is ~ 200 Pa. On the desorption side, first hot oil (H-101) is flowed through the contactors in a 2-fluid system to provide sensible heat. Steam is generated (H-102) and is flowed through the contactors and is condensed at a temperature of 83 ˚C to provide the energy required for desorption. Cooling water is flowed through a condenser (E-101) to condense the water, and the water is separated from the gaseous CO_2 in a knockout drum (V-102). A vacuum pump (P-101) pulls the CO_2 through at a total pressure of 0.5 bar, and exhausts CO_2 at atmospheric pressure.

In this process the contactor bank (comprising 12 contactors) shares a heat exchanger, knockout drum, and vacuum pump. This contactor bank design was used for the PARC DAC and baseline DAC TEA's. The various costs and process parameter assumptions that were used to calculate the capture cost for both the PARC DAC and the baseline DAC case are shown in Table 12.

Table 12: Process parameter assumptions used in the PARC DAC and baseline DAC.

Parameter	Value	Units
Plant lifetime	20	year
Annual production volume	100,000	ton CO_2/year
Uptime	95%	-
Depreciation method	Linear	-
Depreciation period	10	year
Energy source	Wind	-
Cost of electricity	$0.10	$/kWh
Cost of steam	$2.03	$/GJ
Labor cost	$63,640	USD/year
Supervisory labor	$105,550	USD/year
Water treatment cost	$0.16	USD/t water
Boiler efficiency	100%	-
Blower efficiency	70%	-
Contactor volume	2.8	m^3
Sorbent mass per contactor	633	kg

With the process flow diagram established, we then sought to create a cost projection for the PARC adsorbent and to compare the capture cost to one using a baseline adsorbent. The parameters for the PARC and baseline adsorbent are given in Table 13. For the PARC adsorbent, a working capacity of 0.87 mmol/g and an adsorption time of 10 minutes was used. For the baseline adsorbent, a working capacity of 0.3 mmol/g was used. This is consistent with the performance of commercially available weak base anion exchange resins, which are presumably used in the first-generation DAC facilities. The improvement working capacity (and adsorption rate) dramatically reduces the overall capture cost, annual operating cost, fixed capital cost, energy requirement, and plant footprint by reducing the total amount of adsorbent needed in the capture facility.

Table 13: Process Comparison of PARC DAC to Baseline DAC.

Parameter	PARC DAC	Baseline DAC	Units
Adsorption rate	0.087	0.03	mol/kg/min
Adsorption time	10	10	min
Working capacity	0.87	0.3	mol/kg
Desorption time	4.5	1.5	min
Total cycle time	14.5	11.5	min
Contactors per bank	12	12	-
Number of contactor banks	10	22	-
Number of contactors	120	264	-
Number of blower fans	120	264	-

By improving the adsorption rate and working capacity from 0.03 to 0.087 mol/kg/min and 0.3 to 0.87, respectively, the overall scale of the plant is reduced, and the efficiency is improved. For an equivalent plant capacity, the number of contactors and blowers is reduced from 264 to 120, and the number of contactor banks is reduced from 22 to 10, which dramatically reduces OPEX and CAPEX. Even when considering a longer desorption time needed due to the increased amount of CO_2 that needs to be regenerated from a given contactor, the total adsorbent mass that is needed is reduced by 55%. This has knock-on effects on the overall technoeconomics.

Table 14: Total capture cost (excluding storage) comparison for PARC DAC and baseline DAC scenarios.

	PARC DAC	Baseline DAC	Units
Total cost of capture	$170	$419	$/ton CO_2
Capital Expenditure	$17	$39	$/ton CO_2
Sorbent Cost	$96	$278	$/ton CO_2
Other Operating Cost	$16	$23	$/ton CO_2
Utilities cost	$40	$79	$/ton CO_2

Table 15: Annual operating cost comparison for PARC DAC and baseline DAC scenarios.

	PARC DAC	Baseline DAC	Units
Annual operating cost	$14.47	$35.87	$MM
Depreciation	$1.46	$3.33	$MM
Adsorbent	$8.17	$23.83	$MM
Labor	$1.40	$1.97	$MM
Utilities	$3.44	$6.74	$MM

Table 16: Fixed capital investment comparison for PARC DAC and baseline DAC scenarios.

	PARC DAC	Baseline DAC	Units
Fixed capital investment	$15.43	$34.96	$MM
Blower fans	$5.22	$12.08	$MM
Vacuum pumps	$1.45	$5.25	$MM
Contactor arrays	$3.95	$9.14	$MM
Process heat system	$1.43	$1.43	$MM
Packaged steam boiler	$1.27	$2.20	$MM
Steam condensers	$0.45	$1.17	$MM
Knockout drums	$0.15	$0.39	$MM
Working capital	$1.53	$3.36	$MM

The projected capture cost for the PARC DAC scenario is $170/ton CO_2, compared to $419/ton CO_2 for the baseline DAC scenario. This is due to a 60% reduction in the annual operating cost ($14.47M vs. $35.87M) and a 56% reduction in the fixed capital investment ($15.43M vs. $34.96M). The annual operating cost reduction is driven by a reduction in depreciation due to the lower fixed capital investment, a reduction in the sorbent cost due to less sorbent being installed

in the facility and less sorbent needing to be replaced, a reduction in labor due to the smaller scale of the facility with fewer operators needed, and reduction in utilities due to less waste heat being generated during desorption. The fixed capital investment reduction is driven by fewer contactors requiring fewer blower fans and fewer contactor banks requiring fewer of the auxiliary components like vacuum pumps, boilers, condensers, and knockout drums.

Conclusions

The project was successful in advancing the direct air capture technology to TRL 3. The key accomplishments include (1) a demonstration of state-of-the-art adsorbent performance using formulation-optimized PVAm-DVB, (2) a development of a novel structured adsorbent platform using non-woven polypropylene to produce reinforced adsorbent sheets, and (3) a projection of significant CO_2 capture cost reduction resulting from adsorbent performance improvements. TRL 4 and TRL 5 are on the horizon, with the demonstration of contactor and laboratory-scale DAC system performance, respectively.

References

1. Sculley, J. P.; Zhou, H.-C.; *Agnew. Chem. Int. Ed.* 2012, 51 (12660-12661).
2. Veneman, R.; Frigka, N.; Zhao, W.; Li, Z.; Kersten, S.; Brilman, W.; *Int. J. Greenh. Gas. Cont.* 2015, 41 (268-275).
3. Rezaei, F.; Webley, P.; *Chem. Eng. Sci.* 2009, 24 (5182-5191).